

## **SHORT PERIOD SURFACE WAVE DISPERSION ACROSS THE MEDITERRANEAN REGION: IMPROVEMENTS USING REGIONAL SEISMIC NETWORKS**

Michael H. Ritzwoller<sup>1</sup>, Yingjie Yang<sup>1</sup>, Rachelle Richmond<sup>1</sup>, Michael E. Pasyanos<sup>2</sup>, Antonio Villaseñor<sup>3</sup>, Vadim Levin<sup>4</sup>, Rami Hofstetter<sup>5</sup>, Vladimir Pinsky<sup>5</sup>, Nadezda Kraeva<sup>5</sup>, and Arthur Lerner-Lam<sup>6</sup>

<sup>1</sup>University of Colorado at Boulder, <sup>2</sup>Lawrence Livermore National Laboratory, <sup>3</sup>Institute of Earth Sciences “Jaume Almera” - Barcelona, <sup>4</sup>Rutgers University, <sup>5</sup>Geophysical Institute of Israel, <sup>6</sup>Lamont-Doherty Earth Observatory

Sponsored by National Nuclear Security Administration  
Office of Nonproliferation Research and Development  
Office of Defense Nuclear Nonproliferation

Contract No. <sup>1</sup>DE-FC52-05NA26607 [BAA05-48], <sup>2</sup>W-7405-ENG-48 [BAA05-48]

### **ABSTRACT**

We have begun to apply ambient noise surface wave tomography to broad-band seismic data obtained in Europe, North Africa, the Middle East, and Central Asia. The goal is to improve the calibration of surface wave propagation in aseismic areas. Ambient noise tomography (ANT) generates surface wave dispersion maps to periods as short as 6 sec across large areas and, therefore, provides new, high resolution constraints on crustal structures homogeneously over extended regions. Current work concentrates on the application of ANT in Europe where station coverage is highest, which allows improvements in the method to be made rapidly and transported elsewhere later.

In earlier work, we applied ambient noise tomography across Europe to one-year of data from approximately 125 stations composing the Virtual European Seismic Network (VEBSN) (available from the ORFEUS Data Center) to produce Rayleigh wave group velocity maps from 8 – 40 sec period. Current work builds on these results by using longer time series (to improve signal quality and provide measurement uncertainties) and assimilating data from temporary or emerging regional networks in the Mediterranean region to generate Rayleigh wave phase and group speed maps across Europe with better resolution and reliability. The study concentrates on improvements in three focus areas where regional array data are available: (1) the western Mediterranean, particularly the Iberian Peninsula, (2) the central Mediterranean, notably Italy and Switzerland, and (3) the eastern Mediterranean, including Israel, Syria, and Turkey. The western Mediterranean results are based on the Spanish National Network data, which provides much tighter constraints on the crustal structures of the Iberian Peninsula. In the Central Mediterranean, the RETREAT and CAT-SCAN PASSCAL experiments yield data that improve resolution in this area considerably. In the eastern Mediterranean, the Israeli DESERT2000 experiment and the Eastern Turkey PASSCAL experiment were performed simultaneously for an extended time period and, together with other regional stations, greatly improve ray coverage in the region.

We present Rayleigh wave group and phase speed measurements with associated uncertainties (where time series are sufficiently long) and dispersion maps in two of the three focus regions. Resolution and the retrieval of geologically correlated features on the dispersion maps are significantly improved using the regional data.

## **OBJECTIVE**

The goal of this research is to develop a new method to obtain surface wave dispersion measurements based on ambient seismic noise and to produce a new data set of inter-station group and phase velocity measurements. These new data are used to produce group and phase velocity dispersion maps, particularly at periods below about 25 sec.

## **RESEARCH ACCOMPLISHED**

### **Introduction**

Surface wave empirical Green functions (EGFs) can be determined from cross-correlations between long time sequences of ambient seismic noise observed at different stations. The feasibility of the method was first established by experimental (e.g., Weaver and Lobkis, 2001; Lobkis and Weaver, 2001; Derode et al., 2003; Larose et al., 2004, 2005) and theoretical (e.g., Snieder, 2004; Wapenaar, 2004) studies. Shapiro and Campillo (2004) demonstrated that Rayleigh wave EGFs estimated from ambient noise possess dispersion characteristics similar to earthquake derived measurements and model predictions. Bensen et al. (2007a) describe the ambient noise data processing procedure in detail. The dispersion characteristics of surface wave EGFs derived from ambient noise have been measured and inverted to produce surface wave tomography maps in several regions, such as Southern California (Shapiro et al., 2005; Sabra et al., 2005; Gerstoft et al., 2006), the western US (Moschetti et al., 2007; Lin et al., 2007b), Europe (Yang et al., 2007), Tibet (Yao et al., 2006), New Zealand (Lin et al., 2007a), Korea (Cho et al., 2007), Spain (Villasenor et al., 2007) and elsewhere. Ambient noise tomography has also been employed on a continental scale in Europe (Yang et al., 2007) and the US (Bensen et al., 2007b). Most of these studies obtained Rayleigh wave group velocity maps at periods below 20 sec period, but longer period maps up to periods of 70 sec (e.g., Yang et al., 2007; Bensen et al., 2007b), phase velocity maps (e.g., Yao et al., 2006; Lin et al., 2007b), and Love wave maps (e.g., Lin et al., 2007b) have also been developed.

Three publications have resulted from the research supported by this contract: Bensen et al. (2007a), Yang et al. (2007), and Villasenor et al. (2007). Bensen et al. (2007a) describes the data processing procedure that has been developed under this contract. The first ambient noise tomography of the Mediterranean region and Europe was performed by Yang et al. (2007) using one year of continuous seismic data taken predominantly from the Virtual European Broadband Seismic Network (VEBSN) obtained from the Orfeus Data Center in Europe. Attempts to refine the maps of Yang et al. (2007) are based on utilizing regional and national network data that tend not to be available from the major international data centers such as the IRIS-DMC or the Orfeus Data Center. A proof-of-concept study was performed using four months of data from the Spanish National Network and results appear in Villasenor et al. (2007).

The focus of this paper is to report on further attempt to improve upon the first tomographic images provided by Yang et al. (2007) by extending results to phase velocities, improving resolution by introducing more seismic stations predominantly from regional networks and temporary installations, and improving reliability of the measurements and uncertainty estimates by using longer time series. Because the available stations change over time, optimal improvements depend on using data from several years. We currently are working to process data from European seismic stations acquired from various sources recorded during the years 2000 through 2006. Differences in stations operating in 2000-2001 and 2005-2006 are shown in Figure 1. Regional networks such as the Spanish National Network and PASSCAL experiments are important resources. The earlier time periods are important for resolution in the eastern Mediterranean and parts of the Middle East.

### **State of Ambient Noise Data Processing**

The ambient noise data processing procedure is described by Bensen et al. (2007a) in detail, but is summarized here briefly. All data are processed on a daily basis and then are stacked (superposed and added together) later to achieve cross-correlations over arbitrarily long time series currently ranging up to two years. The mean, trend, and instrument response of the daily three-component (E, N, Z) seismograms are removed and the resulting waveforms are band-pass filtered between periods of 5 sec and 100 sec. We now compute the full cross-correlation tensor and

not just vertical-vertical cross-correlations. To speed up the process, we do not rotate the components into the radial (R) and transverse (T) directions for each station-pair until the component cross-correlations (E-E, E-N, N-N, N-E) are performed. Earthquake signals and instrumental irregularities are then removed by temporal normalization. In order to postpone the component rotation until after cross-correlation, the East and North components are temporally normalized together. To achieve this, both components are band-pass filtered between 15 sec and 50 sec, a band that contains the most energetic surface wave signals from earthquakes. For each time point, the mean of the absolute value of each seismogram is computed in the 128 second window centered on that point. The values of the East and North components are compared, and the larger is used to define the inverse weight for that time point. That weight is then applied to both the North and East component time-series, band-passed between 5 sec to 100 sec. This process effectively suppresses earthquake signals and maintains the linearity of the rotation operator. After temporal normalization, the signals are whitened in frequency. Before whitening, ambient noise is most energetic in the microseism bands below 20 sec period. Frequency whitening is carried out to broaden the period band of the dispersion measurement. Again, to maintain the linearity of the rotation operator, the East and North signals are whitened together. Because the spectra of both components are similar, on average, we do this by simply weighting the East and North signals in the frequency domain by the inverse of the smoothed East spectrum. Other methods, such as weighting by the mean of the two spectra or their product, produce similar results. We then stack all available daily cross-correlations for each component and station-pair in order to enhance the signal-to-noise ratio (SNR). Because all of these processes are linear in the rotation operator, the transverse-transverse, transverse-radial, radial-radial, and radial-transverse cross-correlations between each station-pair can be calculated by a linear combination of those four components. The resulting cross-correlations can be converted to Empirical Green's functions by introducing an additive phase factor (Lin et al., 2007b).

Examples of vertical component cross-correlation record sections are shown in Figure 2. Figure 2a is based on four-months of ambient noise data from the Spanish National Network. Figure 2b is from 12-month time series centered on a station in central Italy. The arrivals near zero cross-correlation lag are not interpreted in this study, and their origin remains unknown. We believe that they result from the conversion of ocean waves to mantle propagating P-waves in the European Arctic. They are observed elsewhere across Eurasia, and understanding their generation and nature requires further effort. They do not, however, interfere with the fidelity of the surface wave dispersion measurements.

Yang et al. (2007) processed one year of data from 2004 taken from about 120 stations available from the Orfeus Data Center in Europe. Station coverage was similar to the red symbols shown in Figure 1a.

Improvements over the results of Yang et al. (2007) derive from three factors. First, we will use longer time series, two years of data, which will allow the computation of better measurement uncertainties. Uncertainties are computed from repeating the measurements in different seasons. Second, there are data resources in Europe, North Africa, and the Middle East that were not used by Yang et al. These include national networks such as the Spanish National Network and the Israeli DESERT2000 experiment, PASSCAL experiments such as the RETREAT and CAT-SCAN experiments in Italy and Eastern Turkey and Northern Anatolian Fault (ANF) experiments in Turkey, as well as other temporary deployments such as the Mid-Sea Experiment and the Carpathian Basin Project (CBP) in Austria and Hungary. We are now in the process of acquiring and beginning to process these data. Focus is being placed on three regions: (1) the western Mediterranean, (2) the central Mediterranean, and (3) the eastern Mediterranean. Third, we have extended the measurements to include phase velocities. Lin et al. (2007b) show that phase velocity measurements are more repeatable than group velocities and, thus, have lower uncertainties.

**Western Mediterranean:** Villaseñor et al. (2007) computed cross-correlations between stations within the Spanish National Network (SNN) during July, August, September and October of 2005. Initially, only group velocity tomography maps were obtained, but we have subsequently measured phase velocities from these data. Additionally, group and phase speed measurements were obtained from cross-correlations between VEBSN and GEOFON stations on the Iberian Peninsula (available from Orfeus and IRIS, respectively) operating from April, 2004 to March, 2005.

**Central Mediterranean:** We have augmented the data processing performed by Yang et al. (2007) by computing cross-correlations and obtaining group and phase velocities from one year of continuous data (April, 2004-March, 2005) using the RETREAT and CAT/SCAN PASSCAL experiments in Northern and Southern Italy, the VEBSN,

and MEDNET station data available from IRIS. The addition of data from the two PASSCAL experiments in Italy significantly improves upon the initial results found by Yang et al. (2007).

**The Eastern Mediterranean/Middle East:** We are currently processing data from stations that operated during 2000 and 2001. This data set includes stations from the Eastern Turkey (PASSCAL) Seismic Experiment, the DESERT2000 experiment in Israel, and stations available from IRIS in Western Turkey and Crete.

### **Current Status: Example Group and Phase Velocity Maps**

Figures 3 and 4 present examples of the current state of the group and phase velocity maps across the region of study. The tomographic method of Barmin et al. (2001) has been used. One aspect of this method is that outside the region of high path coverage, the maps revert to the average of the measurements. Thus, the periphery of all of the maps are white because in these regions there are few ray paths. Tomography is performed on a 1 deg x 1 deg grid over the region of study. Figure 5 is a map of sedimentary and crustal thicknesses taken from CRUST2.0, for comparison.

In Figure 3, low velocities on the 10 sec maps reveal the location of major sedimentary basins. The Po Basin in Italy, the North Sea Basin, the Silesian Basin in northern Germany and Poland, the Tyrrhenian and Adriatic Basins surrounding Italy, and the Valencia Trough east of Spain are some examples. The Valencia Trough and the Sub-Pyrenees Basin are seen better in Figure 4. At 25 sec period, the maps reveal information about vertically integrated crustal shear velocities and crustal thickness (the latter particularly in phase velocities that sample deeper than group velocities). Low velocities are associated with thicker crust. Thus, there are low velocities beneath the Betic Mountains in southern Spain, the Alps, the Carpathians, the Dinarides in the Balkans, and the Apennines along the spine of Italy. The Hellenic Arc also appears as low velocities, but probably not because of particularly thick crust there.

### **Expected Continued Improvements**

Figure 6 shows how path coverage has improved with the addition of measurements obtained in Spain using the Spanish National Seismic Network and data from two PASSCAL experiments in Italy (RETREAT, CAT/SCAN). Nevertheless, the high resolution (non-white) regions of the maps in Figures 3 and 4 are mainly within continental Europe. Our goal is to improve data coverage in the Mediterranean Sea, North Africa, and parts of the Middle East. We plan to continue to improve the data set in each of the three regions by increasing the number of stations, and increasing the time duration of ambient noise analysis.

(1) We will improve upon the initial results of Villaseñor et al. (2007) by increasing the time duration of analysis of the Spanish National Network from four months to two years (2005 and 2006). Additionally, we will include in our analysis data from VEBSN, IRIS, MEDNET and other stations operating in Europe during this time period. By tying the Spanish National Network data to VEBSN and other stations, resolution in the western Mediterranean will be improved dramatically.

(2) To improve ray path coverage and resolution in the central Mediterranean we will compute cross-correlations between stations operating during 2005 and 2006, which includes the RETREAT and CAT/SCAN PASSCAL experiments in Italy and the Spanish National Network, as well as VEBSN and other stations located in this region (Fig 1b). These data will result in additional ray coverage across the Mediterranean Sea between Italy and the Iberian Peninsula and between Italy and the Hellenic Arc.

(3) Cross-correlations between stations operating during the years 2000 and 2001 from the Eastern Turkey Seismic Experiment, the DESERT2000 experiment in Israel, and stations available from IRIS in Western Turkey and Crete will yield improved resolution across Turkey, Syria, Israel, and the Eastern Mediterranean.



## **CONCLUSIONS**

Three studies supported by this contract have already been published. Bensen et al. (2007a) described ambient noise data processing in detail and Yang et al. (2007) performed ambient noise tomography for Rayleigh wave group velocities using observatory data in Europe was performed between 10 sec and 40 sec. In addition, assimilation of regional data by Villasenor et al. (2007), notably using the Spanish National Network, established the ability of such data to improve resolution at short periods (6 – 20 sec) when used in concert with observatory data. Further data processing using PASSCAL experiment data in Italy has established similar results in the central Mediterranean region and the data processing methodology has been extended to include phase velocities. In the near future, more regional data will be assimilated into the inversion to improve data coverage and resolution across much of the Mediterranean Sea, in particular in the eastern Mediterranean, including parts of the Middle East and North Africa.

## **ACKNOWLEDGMENTS**

Most of the data used in this research were downloaded either from the IRIS DMC or the Orfeus Data Center. In addition to observatory data, data were obtained from the Spanish National Seismic Network and from two PASSCAL experiments, RETREAT and CAT/SCAN. This research was supported by a contract from the US Department of Energy, DE-FC52-2005NA26607.

## **REFERENCES**

- Barmin, M., M. Ritzwoller, and A. Levshin (2001). A fast and reliable method for surface wave tomography, *Pure Appl. Geophys.* 158(8): 1351–1375.
- Bensen, G. D., M. H. Ritzwoller, M. P. Barmin, A. L. Levshin, F. Lin, M. P. Moschetti, N. M. Shapiro, and Y. Yang (2007a). Processing seismic ambient noise data to obtain reliable broad-band surface wave dispersion measurements, *Geophys. J. Int.* 169: 1239–1260.
- Bensen, G.D., M.H. Ritzwoller, and N.M. Shapiro (2007b). Broad-band ambient noise surface wave tomography across the United States, *J. Geophys. Res.*, *submitted*.
- Cho, K., R. Herrmann, C. Ammon, and K. Lee (2007). Imaging the upper crust of the Korean Peninsula by surface-wave tomography, *Bull. Seism. Soc. Am.* 97(1B): 198–207.
- Derode, A., E. Larose, M. Campillo, and M. Fink (2003). How to estimate the Green's function of a heterogeneous medium between two passive sensors? Application to acoustic waves, *Appl. Phys. Lett.* 83(15): 3054–3056.
- Gerstoft, P., K. Sabra, P. Roux, W. Kuperman, and M. Fehler (2006). Green's function extraction and surface-wave tomography from microseisms in southern California, *Geophys.* 71(4): 123–131.
- Larose, E., A. Derode, M. Campillo, and M. Fink (2004). Imaging from one-bit correlations of wideband diffuse wave fields, *J. Appl. Phys.* 95(12): 8393–8399.
- Larose, E., A. Derode, D. Clorenec, L. Margerin, and M. Campillo (2005). Passive retrieval of Rayleigh waves in disordered elastic media, *Phys. Rev. E*, 72(4): 46,607.
- Lin, F., M. H. Ritzwoller, J. Townend, M. Savage, and S. Bannister (2007a), Ambient noise Rayleigh wave tomography of New Zealand, *Geophys. J. Int.*: doi:10.1111/j.1365-705 246X.2007.03414.
- Lin, F., M.P. Moschetti, and M.H. Ritzwoller (2007b). Surface wave tomography of the western United States from ambient seismic noise: Rayleigh and Love wave phase velocity maps, *Geophys. J. Int.*, *submitted*.
- Lobkis, O. I., and R. L. Weaver (2001), On the emergence of the Green's function in the correlations of a diffuse field, *J. Acous. Soc. Am.* 110, 3011–3017.

Moschetti, M. P., M. H. Ritzwoller, and N. M. Shapiro (2007). Surface wave tomography of the western United States from ambient seismic noise: Rayleigh wave group velocity maps, *Geochem. Geophys. Geosys.*, in press.

Sabra, K. G., P. Gerstoft, P. Roux, W. Kuperman, and M. C. Fehler (2005). Surface wave tomography from microseisms in Southern California, *Geophys. Res. Lett.* 32(14): 717 14,311-14,314.

Shapiro, N., and M. Campillo (2004). Emergence of broadband Rayleigh waves from correlations of the ambient seismic noise, *Geophys. Res. Lett.* 31(7): 1615–1619.

Shapiro, N. M., M. Campillo, L. Stehly, and M. H. Ritzwoller (2005). High-resolution surface-wave tomography from ambient seismic noise, *Science* 307: 1615–1618,

Snieder, R. (2004). Extracting the Greens function from the correlation of coda waves: A derivation based on stationary phase, *Phys. Rev. E.* 69(4): 46,610-46,624.

Villaseñor, A., Y. Yang, M. H. Ritzwoller, and J. Gallart (2007). Ambient noise surface wave tomography of the Iberian Peninsula: Implications for shallow seismic structure, *Geophys. Res. Lett.* 34(11): doi:10.1029/2007GL030164.

Wapenaar, K. (2004). Retrieving the elastodynamic Green's function of an arbitrary in-homogeneous medium by cross correlation, *Phys. Rev. Lett.* 93(25): 254,301.

Weaver, R. L., and O. I. Lobkis (2001). On the emergence of the Green's function in the correlations of a diffuse field, *J. Acoust. Soc. Am.* 110: 2011-3017.

Yang, Y., M. Ritzwoller, A. Levshin, and N. Shapiro (2007). Ambient noise Rayleigh wave tomography across Europe, *Geophys. J. Int.* 168 (1): 259–274.

Yao, H., R.D. van der Hilst, and M.V. De Hoop (2006). Surface wave array tomography in SE Tibet from ambient seismic noise and two-station analysis: I – Phase velocity maps, *Geophys. J. Int.* 166: 732-744.

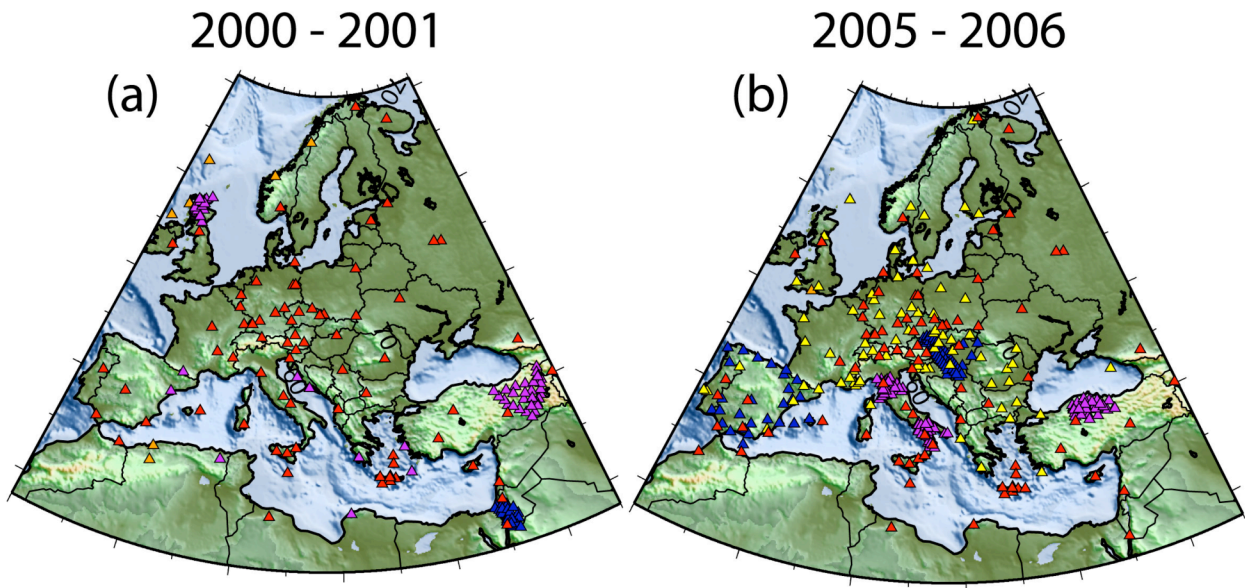


Figure 1. Contrast in station coverage in the years 2000-2001 versus 2005-2006. The station color code is as follows: BLUE - regional networks (e.g., Spanish National Network, the Israeli DESERT2000 experiment); RED - other data available through IRIS; YELLOW - Virtual European Broadband Seismic Network (VEBSN) data available from the Orfeus Data Center in Europe; PURPLE - PASSCAL experiments or other European PASSCAL-like deployments (such as the MIDSEA experiment); ORANGE - SeisUK stations.

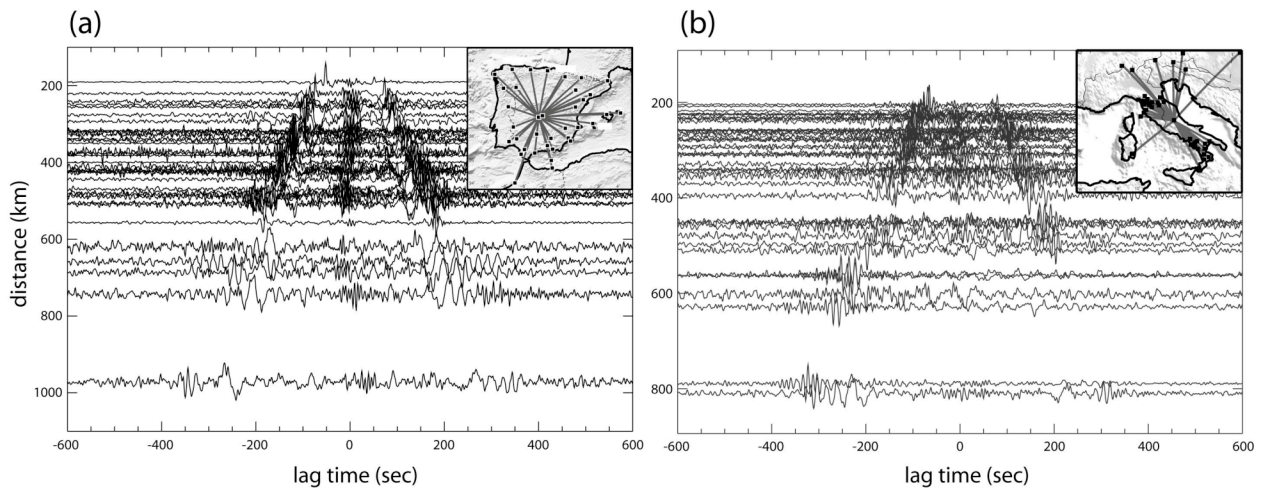


Figure 2. Record sections. (a) From the Spanish National Network. Cross-correlations are from 4-months of data. (b) From stations around Italy. Cross-correlations are from 1-year of data.

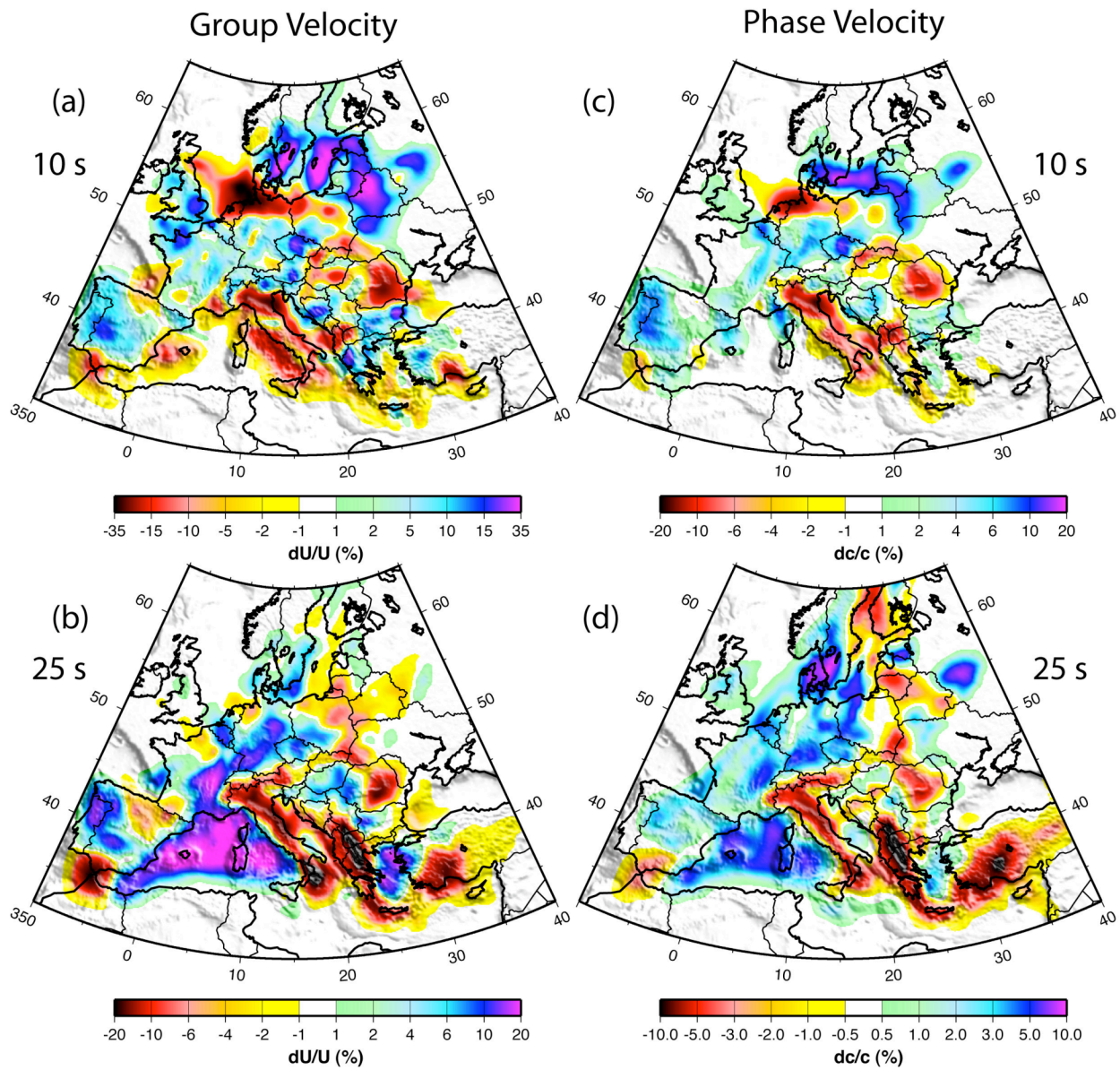


Figure 3. Examples of the current status of Rayleigh wave group and phase velocity maps across Europe. Phase velocities appear in the left column and group velocities in the right column. Maps at 10 sec period are in the top row and at 25 sec period in the bottom row.



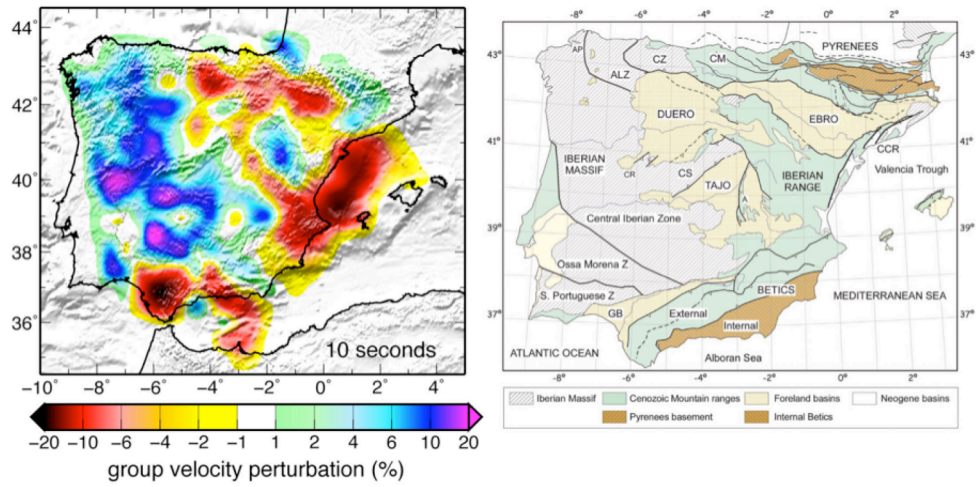
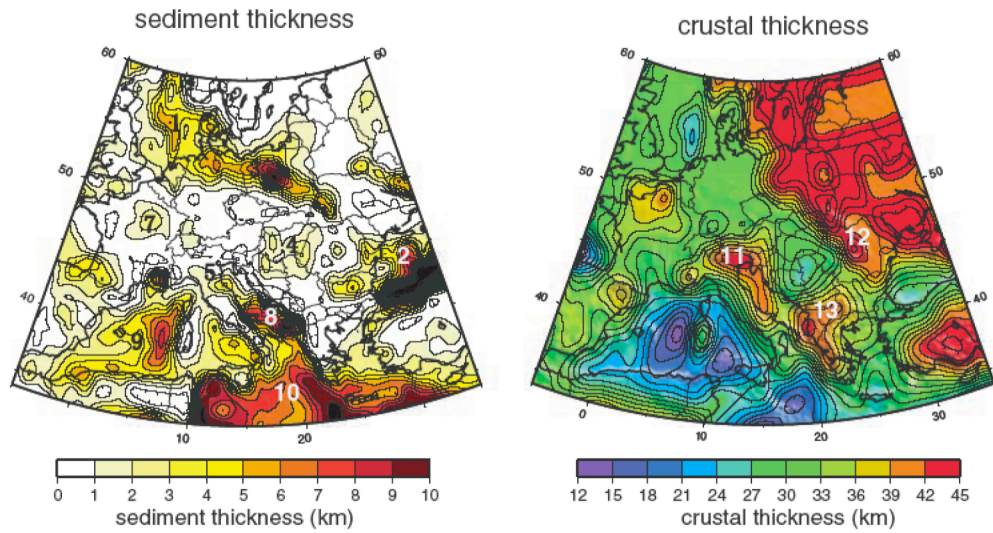


Figure 4. Rayleigh wave 10 sec group velocity map across Spain presented with a tectonic map for comparison. Low velocities are associated with the sub-Pyrenees Basin and the Valencia Trough off-shore. High velocities in the west are associated with the Paleozoic Iberian Massif and the Iberian Range is also correlated with high velocities at this period.



- |                     |                      |                   |                    |
|---------------------|----------------------|-------------------|--------------------|
| 1. North Sea        | 2. Black Sea         | 3. Silesian Basin | 4. Pannonian Basin |
| 5. Po Basin         | 6. Rhone Basin       | 7. Paris Basin    | 8. Adriatic Sea    |
| 9. W. Mediterranean | 10. E. Mediterranean | 11. Alps          | 12. Carpathians    |
| 13. Balkans         |                      |                   |                    |

Figure 5. Sediment thickness and crustal thickness presented for comparison with Figure 4. Values taken from CRUST2.0.

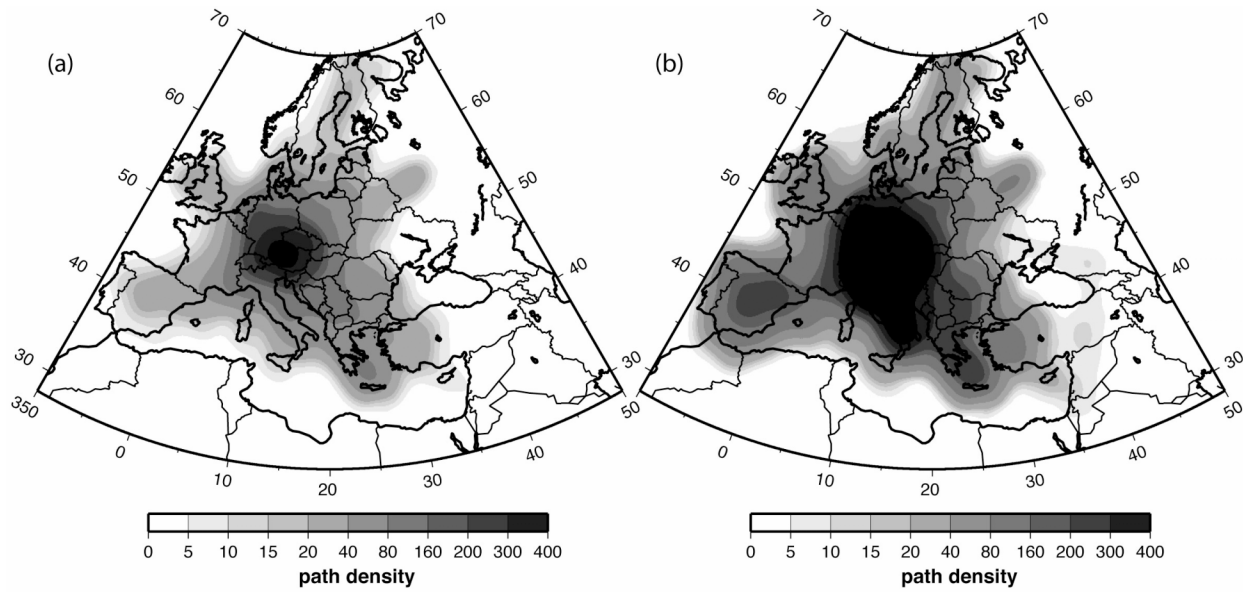


Figure 6. Path density. (a) From the study of Yang et al. (2007). (b) Current state of path density, showing improvements in Spain, central Europe, Italy and the central Mediterranean from recent data processing. Path density is defined as the number of paths intersecting a local 2 deg x 2 deg cell. Addition of more data from other regional networks will improve path density across the entire Mediterranean, particularly in the eastern Mediterranean and parts of the Middle East.